Eur. Polym. J. Vol. 29, No. 6, pp. 809–817, 1993
Printed in Great Britain.

0014-3057/93 $6.00 + 0.00

REGULAR BIMODAL POLYDIMETHYLSILOXANE NETWORKS. ELASTOMERIC PROPERTIES OF THE TETRAFUNCTIONAL NETWORKS

M. A. SHARAF,[1]* J. E. MARK[1]† and Z. Y. AL HOSANI[2]

[1]Department of Chemistry and Polymer Research Center, University of Cincinnati, Cincinnati, OH 45221-0172, U.S.A.

[2]Department of Chemistry, United Arab Emirates University, P.O. Box 17551, Al Ain, United Arab Emirates

(Received 14 August 1992)

Abstract—Regular bimodal tetrafunctional networks of polydimethylsiloxane have been synthesized. The regularity achieved pertains to the specification that each junction in the network be connected to a constant number φ_s of short chains and φ_l of long chains thus giving a value of the network functionality $\varphi_o = \varphi_s + \varphi_l$. The short chains covered a wide range in molecular masses, thus yielding various polydisperse chain length distributions. These networks were studied with regard to their stress–strain isotherms in elongation. Values of the modulus in the large deformation (phantom) limit were found to depend on the chain length distribution. This important result is in disagreement with the phantom network theory, which assumes that the modulus of elasticity is dependent only on a mean value of the chain length, such that the cycle rank of the network is preserved. However, better agreement with experiment, at both limits of deformation, is obtained if the connectivity of the very short chains to the very long ones is taken into account, in what is essentially a bimodal distribution of both network chain lengths and cross-link functionalities.

INTRODUCTION

It is now possible to use endlinking of polymer chains to prepare elastomeric networks having any desired distribution of network chain lengths. The networks so prepared have known structures in that the molecular masses between crosslinks M_n are predetermined as is the distribution of these molecular masses, and the functionality of the crosslinks are known. Endlinking for example has been extensively used in the preparation of model polydimethylsiloxane (PDMS) networks [1–9]. This highly useful technique has been extensively exploited by several groups to obtain experimental evidence for testing the predictions of the theories of rubberlike elasticity. As such, a molecular understanding of rubberlike elasticity is now at a relatively advanced stage.

Bimodal networks having unusual distributions of very short and relatively long chains were also prepared by this technique [10–14]. Model bimodal PDMS networks were first prepared and their elastomeric properties extensively investigated by Mark and coworkers [10–14]. Stress–strain isotherms of such networks showed an anomalous gradual upturn in the modulus at high elongation. Such an increase in modulus constituted the first unambiguous demonstration of non-Gaussian effects related to limited chain extensibilities in non-crystallizable polymer networks [10–14]. These networks are also of practical interest, since they were found to be unusually tough elastomers even in the unfilled state.

It was already observed by Falender *et al.* [15, 16] that the network chain length distribution would have a pronounced effect on both elastomeric properties and effective network functionality. These studies provided interesting information on the effects of segregation of potentially reactive vinyl sites along the chains, and on the selectivity of the crosslinking agent on elastomeric properties [15, 16].

The dependence of elastomeric properties on the network chain length distribution has been the subject of a number of recent investigations. Erman and Mark [17] analysed non-Gaussian behaviour by employing a distribution of end-to-end distances obtained by Fixman and Alben and recommended for short chains. The general shape of the isotherms and its dependence on the number of short chains were reproduced satisfactorily. Higgs and Ball [18] developed a theory for random bimodal networks that essentially describes the fluctuations of junctions as a solution of a nonlinear integral equation. In their formalism, the degree of extension of the network chains differs widely for the long and the short chains. Nonetheless, their results predicted the network modulus to be independent of the polydispersity of the chains. Termonia [19, 20] generated bimodal networks by computer simulation in order to detail the synergism in the elastic properties exhibited by such networks. His study pointed out the importance of the polydispersity index of the short chain components, and the results were in qualitative agreement

*Present address: Department of Chemistry, United Arab Emirates University, P.O. Box 17551, Al Ain, United Arab Emirates; on leave from Cairo University, Beni-Suef, Beni-Suef, Egypt.

†To whom all correspondence should be addressed.

with the experiments of Mark and coworkers [10–14]. Further quantitative investigation of this subject is now in progress by the present authors. In particular, a recent comprehensive investigation by Kloczkowski, Mark and Erman [21] studied the fluctuations of junctions in regular bimodal networks. The regularity in such networks is specified by the requirement that each junction be connected to a fixed number φ_l of long chains and φ_s of short chains.

The present study focuses on synthesizing such regular bimodal networks. Several types of networks with structures that are regular in this sense will be studied. Also, the effects of chain-length distribution will be investigated by having the molecular masses of the short chains cover a wide range, while the molecular mass of the long ones will be fixed. It is the goal of the present study to characterize the effects of such regularity on the elastic behaviour of networks of this type.

STRUCTURAL CONSIDERATIONS AND ELASTICITY EQUATIONS

For a network, the reduced stress or modulus in elongation is defined by [22, 23]

$$[f^*] \equiv f v_2^{1/3}/A^*(\alpha - \alpha^{-2}) \tag{1}$$

where f is the equilibrium force, A^* the original cross-sectional area, $\alpha = L/L_i$ the relative length of the sample (its elongation), and v_2 the volume fraction of polymer during the stress–strain measurements.

Molecular theories of rubberlike elasticity can be divided into two categories: those based on networks which deform affinely (linearly) with the macroscopic deformation, and those based on phantom networks [22, 23]. Both theories are based on simple Gaussian statistics of the network-chain end-to-end distances. In an affine network, fluctuations of the junctions are suppressed by neighbouring chains sharing the same region of space [22, 23]. Consequently, the chain junctions undergo affine displacements, and the reduced stress for a perfect network is given by [22, 23]

$$[f^*]_{\text{aff}} = \nu_a \mathrm{R} T v_{2C}^{2/3} \tag{2}$$

where ν_a is the number of elastically active chains (joined to junctions of functionality $\phi \geqslant 3$), R the gas constant, T the absolute temperature, and v_{2C} the volume fraction of polymer chains in the system being crosslinked which were successfully incorporated in the network structure.

In the phantom network behaviour, which is approached experimentally at high elongations, the chains are assumed to be devoid of material properties, i.e. they can move freely through one another [22–31]. The mean positions of the junctions are affine in the strain, but the fluctuations about the mean positions are invariant with strain. The modulus for this model is given by [22–31]

$$[f^*]_{\text{ph}} = \xi \mathrm{R} T v_{2C}^{2/3} \tag{3}$$

where

$$\xi = \nu_a - \mu_a \tag{4}$$

is the cycle rank of the network, ν_a and μ_a are the number density of the elastically-active chains and junctions, respectively. For a perfect network having functionality ϕ, the cycle rank is expressed as [22–31]

$$\xi = \left(1 - \frac{2}{\phi}\right)\nu_a \tag{5}$$

where the front factor would be $A_\phi = (1 - 2/\phi)$ and the number of active junctions μ_a would be [22–31]

$$\mu_a = (2/\phi)\nu_a = [2/(\phi - 2)]\xi. \tag{6}$$

Therefore, values of the phantom modulus are based only on contributions from active chemical crosslinks.

The role of topology in the phantom network is of great importance. According to Graessley [30–33], the cycle rank of the matrix is the number of cuts required to reduce the network to a spanning tree free of cyclics. This means that the cycle rank would simply depend only on the number of chains and the functionality of the junction ϕ. That is, it would be totally independent of the chain length distribution. It should also be noted here that Graessley later modified equation (5) to (7) [32]

$$\xi = \nu_a - h\mu_a = (1 - 2h/\phi)\nu_a \tag{7}$$

with h being an adjustable parameter between 0 and 1, introduced to take into account possible contributions from interchain entanglements. A consequence of this equation is that the phantom (chemical) modulus would have values different from those predicted from the topology of the chemical crosslinks. More specifically, this equation yields values of the front factor $(1 - 2h/\phi)$ that are generally higher than the values of $(1 - 2/\phi)$ for an idealized phantom network.

The dependence of $[f^*]$ on α is generally represented by the semi-empirical Mooney–Rivlin equation [34, 35]

$$[f^*] = 2C_1 + 2C_2\alpha^{-1} \tag{8}$$

where $2C_1$ and $2C_2$ are constants independent of α [22, 23]. The constant $2C_1$ is thought to approximate the modulus in the high elongation limit of an idealized "phantom" network, where the network junctions undergo very large fluctuations [22–31]. The constant $(2C_1 + 2C_2)$ then approximates the modulus in the limit of very small deformations, where chain-junction entangling suppresses the fluctuations, causing the network chain dimensions to change affinely (linearly) with changes in the macroscopic dimensions of the sample [22, 23]. The constant $2C_2$ is then viewed as representing the decrease in modulus resulting from the deformation becoming increasingly non-affine as the elongation increases [22, 23].

Examples of regular bimodal networks with tetrafunctional junctions are illustrated schematically in Fig. 1(a–c). All junctions have the same functionality ($\varphi_o = 4$) and each junction is connected to the same number φ_l of long chains and φ_s of short chains such that

$$\varphi_o = \varphi_l + \varphi_s. \tag{9}$$

In this study we follow the designations of Kloczkowski *et al.* [21] where regular bimodal networks having i short chains and j long chains at each junction are denoted by S_iL_j.

In Fig. 1(a), the regular bimodal network shown has $\varphi_l = 3$ and $\varphi_s = 1$. All the short and the long chains are assumed to have monodisperse distributions. Here, each junction of the network S_1L_3 is

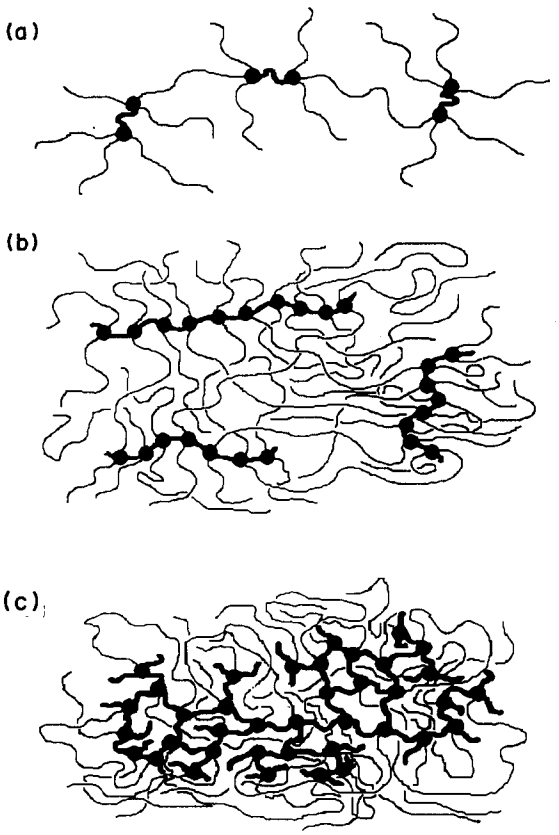

Fig. 1. Sketches showing parts of regular bimodal networks ($\varphi_o = 4$). (a) Shows an S_1L_3 network [in which each junction is connected with one very short (darkened) chain ($\varphi_s = 1$) and three long chains ($\varphi_l = 3$)]. The long chains act as though they were hexafunctionally crosslinked, while the short chains act as though they were tetrafunctionally crosslinked. (b) Illustrates an S_2L_2 network in which the long chains appear to have an effective functionality $\phi_l = \infty$. (c) Represents an S_3L_1 network where the long chains appear to have $\phi_l = \infty$, while the short chains form a three-dimensional network in which they act as though they were tetrafunctionally crosslinked. In all cases, if the connectivity of the very short chains to the long ones is considered, the short chains appear to be tetrafunctionally crosslinked.

attached to one short chain only. As such, the long chains might act as though they are hexafunctionally crosslinked by the short chains ($\phi_l = 6$) while the short chains might act as though they were tetrafunctionally crosslinked. Recent theoretical treatments neglect the connectivity of the long chains to the short ones when studying the behaviour of the short chains in such networks [18, 21]. Accordingly the network represented in Fig. 1(a) is equivalent to a system of free short chains and they are not expected to contribute to the elastic modulus. Such an assumption regarding the connectivity of the short chains is a consequence of the network topology, and is required for the preservation of the cycle rank (which should be independent of the polydispersity of the chain length distribution).

On the basis of connectivity considerations that require the preservation of the cycle rank and neglect the connectivity of the very short chains to the very long ones, the phantom modulus of S_1L_3 network would then be [according to equation (3)] [21]

$$[f^*]_{ph} = (2/3)(3/4)\nu_a RT\nu_{2C}^{2/3} = (1/2)\nu_a RT\nu_{2C}^{2/3} \quad (10)$$

with the effective functionality of the long chains $\phi_l = 6$, and the quantity (3/4) is the mole fraction of the long chains. The net result is that the expected increase in the modulus from the increase of the functionality of the long chains is exactly offset by the decrease in the number of chains [from ν_a to (3/4) ν_a].

However, this analysis is in disagreement with a wealth of experimental evidence on bimodal networks obtained by Mark and coworkers [10–14]. These experiments have shown that the elastomeric properties for bimodal networks are dependent on the mole fraction of the short chains present in the network as well as the ratio of lengths of the short chains to the long ones. Conclusions similar to those of Kloczkowski *et al.* [21] were reached by Higgs and Ball [18] for random bimodal networks. However, it was recognized that this was in discord with experiment [18].

The present authors [36–38], on the other hand, focused attention on the short chain segments between the junction points along the crosslinking molecules and their connectivity to the long network chains. Such segments were found to act as short network chains, thus giving, inadvertently, a strongly "*regular*" bimodal distribution of both the network chain lengths and crosslink functionalities. The interesting point here is that the networks investigated were presumed to be unimodal. When the connectivity of the short chains to the long ones was taken into account, they were found to contribute synergistically to the elastic modulus. Reexamination of some of the published results on this basis provided a reasonable explanation for their unexpectedly high values of the elastic moduli, and also for other experimental observations [36–38]. When the connectivity of the very short chains to the long ones was considered in these revised interpretations, the phantom modulus became the sum of contributions from both the long and short chains [36–38]:

$$\begin{aligned}[f^*]_{ph} &= [f^*]_{long} + [f^*]_{short} \\ &= (1 - 2\phi_l)\nu_a RT\nu_{2C}^{2/3} \\ &\quad + (1 - 2/\phi_s)2\nu_a RT\nu_{2C}^{2/3} \end{aligned} \quad (11)$$

where ϕ_l is the average effective functionality associated with the long chains and ϕ_s is that associated with the short ones. The effective value of $[f^*]_{ph}$ thus increases significantly from what would be expected from network connectivity considerations alone. However, as the short chain length increases, values of the modulus approach those calculated on the basis of the network topology and the cycle rank is preserved [36–38]. The synergism thus observed showed strong dependence on the ratio of the chain lengths of the short chains to the long ones. Consequently, the results are at variance with connectivity considerations discussed above which require the preservation of the cycle rank, regardless of the network chain length distribution or any changes in the effective functionality sensed by the long network chains.

The disagreement could be plausibly attributed to the widely different end-to-end vector distributions

of the long and short network chains. Therefore, the response of the different chains to the extension, and thus their contributions to the modulus will vary. This is, of course, of considerable importance with regard to interpretation of the experimental results.

The relevant theoretical models are based on the approximation of a monodisperse Gaussian distribution [18, 21]. If the short chains, on the other hand, are considered to be elastically effective chains and their connectivity to the long ones is taken into account, then the phantom modulus according to equation (10) would be [36–38]

$$[f^*]_{ph} = (1 - 2/\phi_l)(3/4)\nu_a RTv_{2C}^{2/3} + (1 - 2/\phi_s)(1/4)\nu_a RTv_{2C}^{2/3} = (5/8)\nu_a RTv_{2C}^{2/3} \quad (12)$$

with the value of the front factor A_ϕ increasing by a factor of 1.25 [from (1/2) to (5/8)].

The S_2L_2 and S_3L_1 networks are represented in Fig. 1 (b and c, respectively). The junctions in such networks are attached to more than one short chain. As a result, the network functionality becomes large, with $\phi_l \to \infty$. In the S_2L_2 network, the short chains were considered as equivalent to a single long chain composed of short subchains. Neglecting the connectivity of the short chains to the long ones in the S_3L_1 network would make the network equivalent to a trifunctional network of short chains. The corresponding phantom moduli for these S_2L_2 and S_3L_1 networks would be [21]

$$[f^*]_{ph} = (1/2)\nu_a RTv_{2C}^{2/3} \quad (13)$$

$$[f^*]_{ph} = (1/4)\nu_a RTv_{2C}^{2/3} + (1/3)(3/4)\nu_a RTv_{2C}^{2/3} = (1/2)\nu_a RTv_{2C}^{2/3} \quad (14)$$

respectively. Again, an increase in the functionality of the long chains is offset by reduction in the functionality of the short chains and the number of elastically effective chains.

If the short chains are considered to be elastically effective and their connectivity to the long ones is considered, the phantom modulus for the S_2L_2 networks would be [36–38]

$$[f^*]_{ph} = (1/2)\nu_a RTv_{2C}^{2/3} + (1/2)(1/2)\nu_a RTv_{2C}^{2/3} = (6/8)\nu_a RTv_{2C}^{2/3} \quad (15)$$

and for the S_3L_1 networks

$$[f^*]_{ph} = (1/4)\nu_a RTv_{2C}^{2/3} + (1/2)(3/4)\nu_a RTv_{2C}^{2/3} = (5/8)\nu_a RTv_{2C}^{2/3}. \quad (16)$$

Again, the modulus increases by a factor of 1.5 for the S_2L_2 network, and by a factor of 1.25 for the S_3L_1 network.

Following the same arguments that the connectivity of the short chains to the long ones is neglected for networks having initial $\varphi_o = 3$, the S_1L_2 network would become effectively a unimodal tetrafunctional network composed of long chains only, and the S_2L_1 network effectively a high-functionality one. In turn, the phantom modulus for both networks would be given by [21]

$$[f^*]_{ph} = (1/3)\nu_a RTv_{2C}^{2/3}. \quad (17)$$

However, if the connectivity of the very short chains to the long ones is considered, the phantom modulus for the S_1L_2 and the S_2L_1 networks would be [36–38]

$$[f^*]_{ph} = (1/2)(2/3)\nu_a RTv_{2C}^{2/3} + (1/3)(1/3)\nu_a RTv_{2C}^{2/3} = (4/9)\nu_a RTv_{2C}^{2/3} \quad (18)$$

$$[f^*]_{ph} = (1/3)\nu_a RTv_{2C}^{2/3} + (1/3)(2/3)\nu_a RTv_{2C}^{2/3} = (5/9)\nu_a RTv_{2C}^{2/3} \quad (19)$$

respectively. Thus, when the short chains are considered to be elastically effective, the moduli for the S_1L_2 and S_2L_1 networks increases by a factor of (4/3) and (5/3), respectively.

Of particular importance is the ratio $[f^*]_b/[f^*]_u$. The numerator is the modulus calculated on the assumption that the high-functionality networks are bimodal in both chain-length distribution and crosslink functionality, and the denominator on the assumption that these networks have simple unimodal distributions in long chains only. Values calculated from the above equations are shown as a function of the number of short chains in Fig. 2.

In the affine limit of deformation, the topology of the network is irrelevant and the modulus would be given by equation (2) [22, 23]. However, if arguments neglecting the connectivity of the short chains to the long chains are still valid in this limit, values of the affine modulus so calculated would be less than those predicted according to the present analysis, and they would be given by

$$[f^*]_{aff} = (3/4)\nu_a RTv_{2C}^{2/3}$$
$$[f^*]_{aff} = (1/2)\nu_a RTv_{2C}^{2/3}$$
$$[f^*]_{aff} = \nu_a RTv_{2C}^{2/3} \quad (20)$$

for the S_1L_3, S_2L_2 and S_3L_1 networks, in the same order.

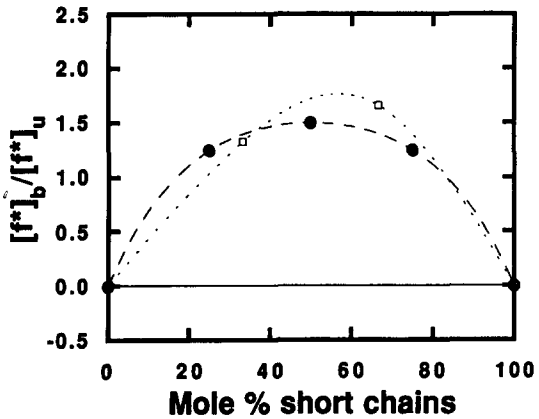

Fig. 2. The ratio $[f^*]_b/[f^*]_u$ of the value of the phantom modulus calculated on the assumption that such networks have a bimodal distribution of crosslink functionality (as described in the text) to the value calculated on the assumption that these polydisperse chains have a unimodal unifunctional distribution of the long chains only. The values are shown as a function of the mole % of short chains. The dashed line represents results for the networks having $\varphi_o = 4$ and the dotted one for those having $\varphi_o = 3$. The solid line represent results calculated with total neglect to any contributions from the short chains.

In this investigation, it is important to emphasize the essential difference between the number ν_a of "*active*" chains (commonly used for imperfect networks), and the number of elastically "effective" chains ν (appearing in most elasticity theories). It is worth noting that, in general, $\nu \neq \nu_a$ [29]. Flory has shown that the number density of elastically effective chains for networks of any kind is given by the universal form [39] $\nu = 2\xi$, with $\xi = \nu - \mu$. As has been pointed out, the identification of ν_a with ν is proper only for perfect networks; otherwise, it is an approximation that is acceptable only for high-functionality networks. With this in mind, the values of ν_a determined by branching theory were used as an approximate substitute for ν in the present investigation. Accordingly, it follows that

$$[f^*]_{\text{aff}} = \nu RT v_{2C}^{2/3} = 2\xi RT v_{2C}^{2/3} \tag{21}$$

and

$$[f^*]_{\text{ph}} = \xi RT v_{2C}^{2/3} \tag{22}$$

with $\xi = \nu_a - \mu_a = \nu - \mu$ [39].

EXPERIMENTAL PROCEDURES

The silanol-terminated bifunctional polymers used in this study were obtained from Petrach Chemicals. Standard fractional precipitation techniques were carried out at 25° on several samples having different molecular masses. Methyl ethyl ketone was chosen as the solvent and methanol as the nonsolvent. Our primary aim for carrying out this procedure was to decrease the polydispersity index of these bifunctional oligomers and to remove the unreactive materials (typically cyclics) usually present in commercial PDMS samples. Such samples appear to have 2–5% impurities of 300–1500 molecular mass. Initial polymer concentrations were about 5%, except for the 25% used for one very low molecular weight sample (Petrach, 15–35 centistokes). The non-solvent also had to be different for this sample, and was an 80/20 methanol/water mixture.

The samples thus fractionated were exhaustively dried under vacuum at 70° for three days. All samples were then stored over molecular sieves to remove any traces of moisture. Their molecular masses and the polydispersity index were obtained by size exclusion chromatography (SEC) using polydimethylsiloxane standards. The polydispersity index $\bar{M}_w/\bar{M}_n$ was generally below 1.3 in all cases except for the lowest molecular mass sample, where it was 1.5. A series of polymers ranging in molecular masses from 710 to 10,600 was utilized to prepare the networks. An additional sample of tetra ethylene glycol having $\bar{M}_n$ of 194 was used to obtain networks having bimodal distributions with exceedingly short chains.

The bimodal networks were prepared in bulk by mixing the precursor chains with tetraethylorthosilicate (TEOS), which was used as received without further purification. The stoichiometry was controlled to achieve a fixed fraction of long and short chains at each junction. The catalyst, stannous 2-ethylhexanoate, was present in amounts corresponding to 0.5% by weight of polymer, and the crosslinking reaction was allowed to proceed in a glove box under N_2.

The first step involved prereacting the precursor chains present in the smaller amount, in order to facilitate regularity of the bimodal chain length distribution around each junction. A third of the total required amount of catalyst was employed, and the reaction was allowed to proceed for about 5 hr before the rest of the stoichiometric balance was added. In no case was gelatin observed at this stage. After this second addition, the samples were placed into suitable moulds and permitted to cure for three days. The networks thus prepared were removed and turned over to facilitate removal by byproducts. They were then allowed to cure further under vacuum for two additional days at 60°. Since only small amounts of the fractionated polymers were available, most networks weighed only about 1.5 g.

The crosslinked sheets were extracted in toluene for one week to remove any unreacted material; the solvent was changed once after the first two days. The networks, after such extraction, were slowly deswollen in a series of toluene-methanol mixtures of increasing methanol content, and then dried under vacuum. The amounts of extracted material (ω_s) were <2.5% for most of the networks. Values of the related quantity, ν_{2C}, the volume fraction of the polymer successfully incorporated in the network structure, are given in Table 1.

Table 1. Elastomeric properties of tetrafunctional regular bimodal networks

Network	$10^{-3}M_n$(s)[a] (g mol^{-1})	$10^{-3}M_n$[b] (g mol^{-1})	ω_s[c]	P[d]	ν_2[e]	ν_{2m}[f]	$\nu_a RT$[g] (N mm^{-2})	$2C_1$ (N mm^{-2})	$2C_2$ (N mm^{-2})	G (N mm^{-2})	$G/\nu_a RT$
S_1L_3											
1	0.194	8.00	0.0131	0.893	0.799	0.301	0.221	0.187	0.094	0.281	1.27
2	0.710	8.13	0.0164	0.882	0.779	0.309	0.208	0.182	0.114	0.296	1.42
3	3.40	8.80	0.0134	0.892	0.797	0.268	0.200	0.111	0.087	0.198	0.99
4	5.40	9.30	0.0190	0.875	0.764	0.255	0.174	0.089	0.103	0.192	1.10
5	7.20	9.75	0.0154	0.885	0.784	0.273	0.175	0.111	0.130	0.241	1.38
6	8.90	10.2	0.0203	0.871	0.757	0.263	0.158	0.075	0.069	0.145	0.92
S_2L_2											
1	0.194	5.40	0.0097	0.906	0.825	0.300	0.343	0.193	0.133	0.326	0.95
3	3.40	7.00	0.0244	0.861	0.739	0.229	0.216	0.183	0.129	0.312	1.45
4	5.40	8.00	0.0132	0.893	0.798	0.308	0.220	0.187	0.144	0.331	1.51
5	7.20	8.90	0.0143	0.889	0.791	0.307	0.194	0.166	0.163	0.328	1.69
6	8.90	9.75	0.0109	0.902	0.814	0.000	0.187	0.161	0.148	0.308	1.65
S_3L_1											
1	0.194	2.80	0.0080	0.914	0.841	0.294	0.679	0.193	0.086	0.279	0.41
2	0.710	3.18	0.0489	0.817	0.664	0.301	0.361	0.167	0.113	0.280	0.77
3	3.40	5.20	0.0224	0.865	0.749	0.335	0.298	0.252	0.134	0.386	1.30
4	5.40	6.70	0.0161	0.883	0.781	0.317	0.251	0.200	0.118	0.318	1.26
5	7.20	8.05	0.0273	0.854	0.727	0.309	0.182	0.155	0.169	0.324	1.79
6	8.90	9.32	0.0241	0.862	0.740	0.312	0.163	0.099	0.286	0.384	2.36

[a]Molecular mass of the short chains.
[b]Molecular mass of the long chains.
[c]Sol fraction.
[d]Extent of reaction, as determined by branching theory [7, 8, 40].
[e]Volume fraction of elastically effective chains, as determined by branching theory [7, 8,40].
[f]Volume fraction of polymer at equilibrium swelling in toluene at 25°.
[g]Number density of elastically effective chains multiplied by RT, as determined by branching theory [7, 8, 40].

Stress–strain isotherms were obtained on strips cut from the various network sheets. The central test portions of the strips had lengths of about 4.5 cm, widths of about 0.4 cm, and thicknesses of 0.7–1.2 mm. The elongation was measured using four fiducial marks, nearly 0.75 cm apart. Stress–strain measurements were obtained using a sequence of increasing values of the elongation $\alpha = l/l_o$. Some measurements were taken out of sequence to test for reversibility. The isotherms were, in general, found to be reversible. In fact, in previous studies, bimodal networks with very high proportions of short chains gave highly reversible results for the entire isotherms [10–14]. Generally, the test specimens did not break but in most of the cases slipped from the clamps. This was tolerable, since ultimate properties were not the primary concern of the investigation.

RESULTS AND DISCUSSION

The stress–strain data were interpreted in terms of the reduced stress or modulus, as defined in equation (1). The equilibrium values of $[f^*]$ were plotted against the reciprocal elongation α^{-1} as suggested by the Mooney–Rivlin procedure, embodied in equation (8). The straight lines through the isotherms were located by least-squares analysis. The stress–strain isotherms are illustrated in Figs 3–5 for S_1L_3, S_2L_2, S_3L_1, respectively. Values of the constants $2C_1$ and $2C_2$ thus obtained are reported in Table 1.

Values for the extent of reaction P, number of elastically active chains ν_a, and the volume fraction of the elastically effective chains v_2 were calculated from the sol fraction ω_s using branching theory [7, 8, 40]; they are listed in Table 1. The experimental moduli at large and small strains were calculated from equation (1). The small-strain modulus $[f^*]_{aff}$ was identified with the shear modulus $G = 2C_1 + 2C_2$, and the phantom modulus $[f^*]_{ph}$ with $2C_1$. As already mentioned, the constant $2C_2$ is a measure of the change in modulus for the transition between the two extremes of deformation [22, 23]. It should be noted that values of $2C_1$ usually slightly overestimate $[f^*]_{ph}$ due to the lengthy extrapolation required from the moderate-strain region covered in most experiments. It should also be noted that dangling ends as well as other network imperfections could act as diluent [41].

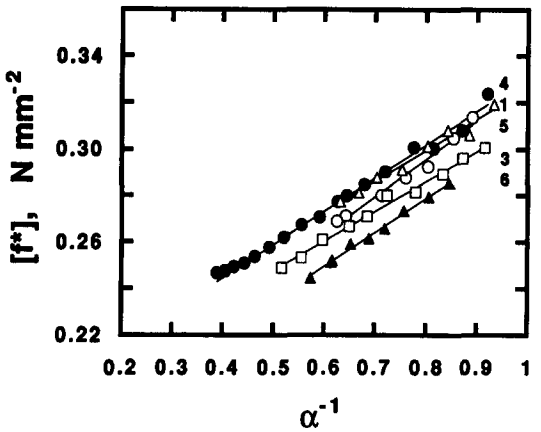

Fig. 4. Stress–strain isotherms obtained on the regular bimodal S_2L_2 networks; see legend to Fig. 3.

Consequently, the factor $v_2^{-1/3}$ representing the volume fraction of elastically ineffective chains should be incorporated, even for networks studied in the dry unswollen state. Thus, more accurate values of the moduli would be obtained according to the equations

$$[f^*]_{aff} = \nu_a RT(V/Vo)^{2/3}v_2^{-1/3} \quad (23)$$

$$[f^*]_{ph} = \xi RT(V/Vo)^{2/3}v_2^{-1/3} \quad (24)$$

Values of the large deformation modulus $2C_1$ are plotted in Fig. 6 against the active chemical degree of crosslinking ν_a multiplied by RT. Such a plot includes the results obtained for the three types of networks, namely S_1L_3, S_2L_2 and S_3L_1. Filled circles represent results for the S_1L_3 networks, open circules for the S_2L_2 ones, and open triangles for the S_3L_1 ones. In every case, the molecular mass of the long chains was 10,600 g/mol. The solid line represents theory, according to which the ordinate should equal the abscissa. In other words, it would represent the network connectivity as determined from the phantom network topology, according to equation (24). As discussed previously, the most recent theoretical models preserve the connectivity (the cycle tank) of the network regardless of chain length distribution [18, 21].

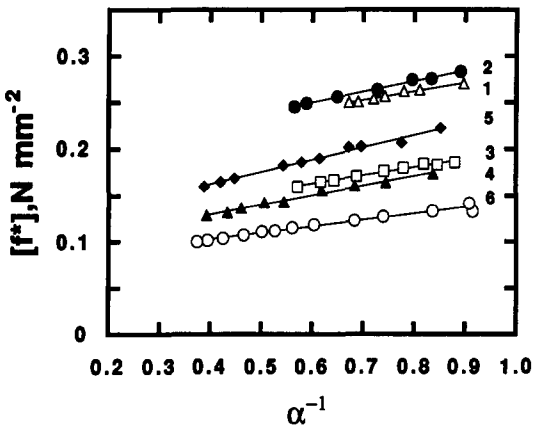

Fig. 3. Stress–strain isotherms obtained on the regular bimodal S_1L_3 networks in elongation at 19°. Each isotherm is labelled according to its designation in Table 1.

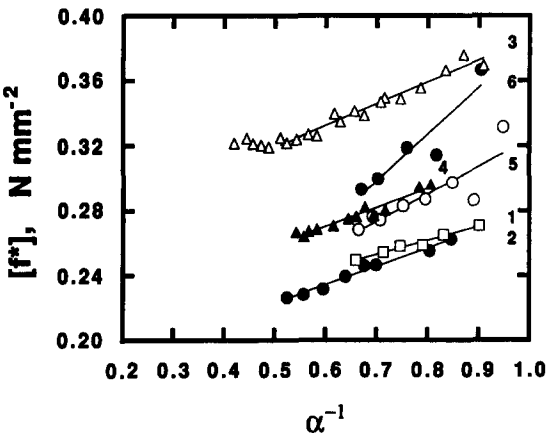

Fig. 5. Stress–strain isotherms obtained on the regular bimodal S_3L_1 networks; see legend to Fig. 3.

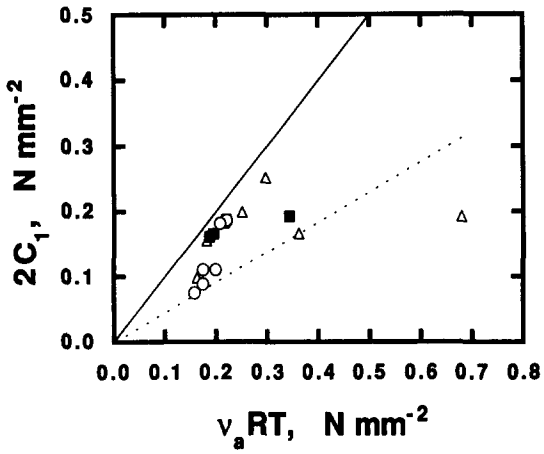

Fig. 6. The phantom modulus, as approximated by $2C_1$, shown as a function of the degree of crosslinking $\nu_a RT$ as obtained from the end-linking chemistry. The circles represent results obtained for the S_1L_3 networks, the filled squares for S_2L_2 ones, and the triangles are for the S_3L_1 ones. The dotted line represents results calculated for the phantom modulus based on the unimodal representation of the networks, i.e. with total neglect of any contributions from the short chains, according to equation (24). The solid line represents the results for the affine modulus according to which the ordinate should equal the abscissa, calculated according to equations (21) and (23).

This is generally achieved by having the polydisperse chains correspond to an average chain length. At intermediate values of the chemical degree of interlinking, variation in values of $2C_1$ is clearly demonstrated within limits set by the inherent inaccuracies in the Mooney–Rivlin analysis. Thus, the results suggest a strong effect of the network chain length distribution on the observed values of the phantom modulus, as identified by $2C_1$. At relatively high and low values of $\nu_a RT$, however, the values of $2C_1$ approach those predicted from the simple network connectivity.

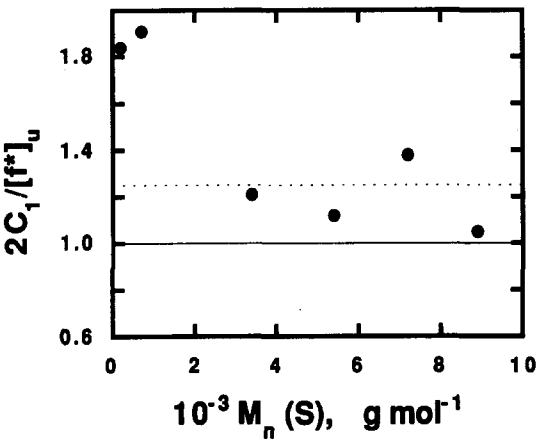

Fig. 7. Values of ratio $2C_1/[f^*]_u$ for the S_1L_3 networks shown as a function of the molecular mass M_n(s) of the short chains. The denominator was calculated from equation (24), on the assumption that these networks have simple unimodal distributions (as described in the text).

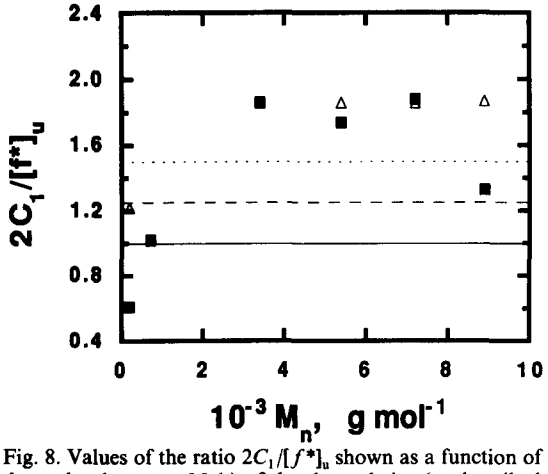

Fig. 8. Values of the ratio $2C_1/[f^*]_u$ shown as a function of the molecular mass M_n(s) of the short chains (as described in the text). The triangles represent results obtained from the S_2L_2 networks, and the filled squares are for the S_3L_1 ones. See legend to Fig. 7.

This phenomenon is explored further in Fig. 7, where the property of primary interest is the ratio $2C_1/[f^*]_u$. The numerator is the experimentally determined phantom modulus as identified by $2C_1$, and the denominator was calculated on the assumption that these networks have simple unimodal unifunctional distributions of the long chains. The ratio is shown as a function of the molecular weight M_n(s) of the short chains. Average values of M_n that corresponds to an average chain length distribution are reported in Table 1. If the phantom modulus were independent of the chain length distribution, this ratio should have remained unity, corresponding to the solid line. As discussed above, values of the phantom modulus, calculated on the assumption that these S_1L_3 networks have a bimodal distribution of crosslink functionalities ($\phi_l = 6$ and $\phi_s = 4$), should increase by a factor of 1.25, as represented by the dotted horizontal line. As already mentioned, consideration of the connectivity of the very short chains violates preservation of the cycle rank. However, within the observed scattering exhibited in Fig. 7, the results support the taking into account of the connectivity of the very short chains in what would essentially be a bimodal bifunctional network. Thus, the results show an unambiguous dependence of elastomeric properties on network chain-length distribution. The ratio $2C_1/[f^*]_u$ decreases with an increase in values of M_n(s) of the short chains, and approaches the expected value of unity. As expected, all the chains would have nearly equal lengths, to the extent that the network would appear to be unimodal with $\phi = 4$.

The pertinent results for the S_2L_2 and the S_3L_1 networks are shown in Fig. 8. Although there is a great deal of scatter, the ratio $2C_1/[f^*]_u$ at least qualitatively follows the expected trend based on the connectivity of the very short chains to the long ones. Within the limits imposed by the scatter, there is satisfactory agreement with our predictions that this ratio should approach 1.5 for the S_2L_2 network and 1.25 for the S_3L_1 network. Particularly to be noted here is the lower values of $2C_1/[f^*]_u$ obtained at small values of M_n(s). Such networks having a high

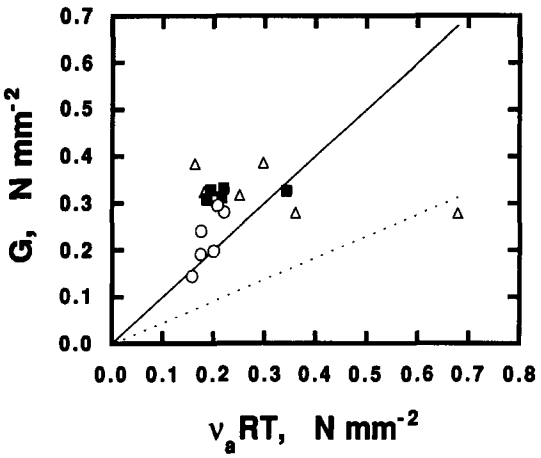

Fig. 9. The shear modulus G for the regular bimodal networks, as approximated by $2C_1 + 2C_2$, shown as a function of $\nu_e RT$. See legend to Fig. 6.

percentage (*ca* 75 mol%) of short chains approach the phantom behaviour of a network composed of very short chains. This is different from the situation with the S_1L_3 networks, where the number of short chains is far smaller (*ca* 25 mol%).

It is to be noted here that the experimental values so interpreted are somewhat larger than the upper limit predicted by our models. Such an enhancement has been observed to vanish upon swelling, suggesting that it is due to difficulties in reaching elastic equilibrium when the network chains are very long [6, 22]. This could also be due to higher slopes in Mooney–Rivlin curves for samples with high molecular mass M_n between crosslinks, which makes the lengthy extrapolation to $\alpha \to \infty$ less reliable [21]. Also of relevance here is the fact that small changes in the sol fraction reflect large variations in the number of elastically active chains ν_a, as determined from branching theory [7, 8].

An additional important difficulty, inherent in the siloxane system, is the possibility of hydrolysis of some of the TEOS, resulting in the formation of reinforcing silica-like particles [42]. Finally, it has recently been reported that the catalyst stannous 2-ethylhexanoate, much used to catalyse the hydrolysis reaction, will also catalyse chain extension of the hydroxyl-terminated PDMS [43]. In this case, the actual value of M_n between crosslinks could be higher than that for the precursor chains.

It is useful to interpret the data in the small deformations (affine) limit. In Fig. 9, values of G (as approximated by $2C_1 + 2C_2$) are plotted against values of νRT. The solid line represents theory in which the affine modulus for a bimodal network is given by equation (23). The dotted line shows values of the phantom modulus $[f^*]_{ph}$ calculated according to equation (24). The data, so represented, do not unambiguously suggest an appreciable intercept with the ordinate.

The enhancement of $[f^*]$ in this limit ($\alpha \to 1$) could be due to any of the reasons cited above. The interesting point here is that, at higher values of νRT, values of G tend towards the phantom limit of the modulus. Again, actual values of G predicted by the constrained junction theory should fall below the upper bound even at small strains [10, 22]. Such behaviour is essentially due to the decrease in the degree of interpenetration with an accompanying decrease in the severity of the constraints on the fluctuation of junctions [10, 22]. Analyses based on the constrained junction theory allow for such a decrease in the degree of interpenetration as the network chain length decreases [26–29]. The broken line in Fig. 9 represents calculations based on the constrained junction model, calculated according to equations reported elsewhere [22, 23, 28]. Extrapolations in the region where the affine to phantom transition ensues amount to placing a single straight line through two line segments of different slope. This, not surprisingly, generally yeilds a substantial intercept on the ordinate [7, 8]. Because of this alternative interpretation, it may be misleading to attribute the intercept to contributions from trapped entanglements [7, 8].

Most of the results presented here concerned model networks that are assumed to be perfect. Nevertheless, networks so prepared may be somewhat imperfect due to possibly inaccurate stoichiometry and/or other conditions that would lead to incomplete crosslinking. Also, as has been mentioned before, it may be difficult to obtain accurate values of the sol fraction and from them the structural parameters of the network. A last difficulty could arise from inhomogeneities in the crosslinking process, as has been pointed out [48]. A straight-forward method for testing the validity of the predictions of the theory of Flory and Erman consists of plotting $G \approx 2C_1 + 2C_2$ against $2C_1 \approx [f^*]_{ph}$ in order to overcome the cited difficulties in obtaining accurate values of the structural parameters of the network. As previously discussed, $2C_1$ can be identified with $[f^*]_{ph}$, within limits set by inherent inaccuracies in the Mooney–Rivlin procedure [41]. According to theory [33–36], $[f^*]_{ph}$ in any network is proportional to the effective interconnectivity of the network and, therefore, can be used to define an effective number of chains ν and junctions μ, regardless of how incomplete the network formation. The results thus

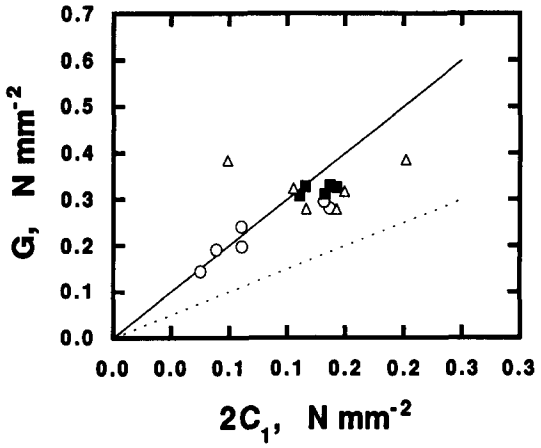

Fig. 10. The modulus shown as a function of the Mooney–Rivlin estimate of the high-deformation modulus. The solid line is for the affine limit for an imperfect network as approximated by $2(2C_1)$, calculated from equation (25). The dashed line is for the phantom modulus approximated by $2C_1$ itself. See legend to Fig. 6.

obtained are plotted in Fig. 10. The dashed line represents the lower bound of the theory (the phantom limit). The solid line approximates the upper bound (the affinely-deforming network), calculated from equations (21) and (23), proposed by Flory [39] for imperfect networks:

$$[f^*]_{\text{aff}} = \nu RT v_{2C}^{2/3} = 2\xi RT v_{2C}^{2/3} = 2(2C_1). \quad (25)$$

The results are well represented within the two limits of deformation. Again, as the degree of crosslinking is increased, there appears to be a trend toward the lower bound (the phantom limit). As has been pointed out, this is expected since the constraints on the fluctuations of the junctions vanish with an increase in either the degree of crosslinking or the deformation. The results, so portrayed, argue against contributions to the small-strain modulus from trapped entanglements. The present procedure circumvents difficulties in accurately determining chain molecular masses and functionalities. As noted above, these difficulties can lead to inaccuracies in the determination of the network parameters, as well. Thus, the results are in accord with the main premises of the constrained junction theory and the universal treatment of imperfect networks set forward by Flory [39]. If the connectivity of the very short chains to the very long ones is ignored, values of the affine modulus calculated for the S_1L_3 and the S_2L_2 networks, according to equation (20), would be lower than those predicted according to equation (2). Apparently, this is not the case, more specifically at lower to intermediate values of νRT. As such, the results so presented in Figs 9 and 10 are consistent with our postulations that take into account the connectivity of the very short chains to the very lone ones.

In any case, it does seem necessary to take into account the connectivity of the very short network chains to the long ones in what is essentially a bimodal bifunctional network. In particular, the results demonstrate a significant dependence of the phantom modulus on network chain length distribution. This dependence calls into question the basic assumption of the phantom network theory that the cycle rank is to be preserved regardless of the polydispersity of the chains. Finally, it is clear that accurate measurements of the network structural parameters are absolutely essential in order to test the molecular theories of rubberlike elasticity.

Acknowledgments—It is a pleasure to acknowledge the financial support provided by the National Science Foundation through Grant DMR 89-18002 (Polymers Program, Division of Materials Research). Our thanks are extended to Professor S. J. Clarson for his invaluable assistance in the GPC measurements and for some helpful comments. We are also indebted to Dr A. Kloczkowski and Professor B. Erman for several very helpful discussions.

REFERENCES

1. J. E. Mark. *Adv. Polym. Sci.* **44,** 1 (1982).
2. J. E. Mark and J. L. Sullivan. *J. Chem. Phys.* **66,** 1006 (1977).
3. J. E. Mark, R. R. Rahalkar and J. L. Sullivan. *J. Chem. Phys.* **70,** 1749 (1979).
4. M. A. Llorente and J. E. Mark. *Macromolecules* **12,** 673 (1979).
5. M. A. Llorente and J. E. Mark. *Macromolecules* **13,** 681 (1980).
6. B. Erman and P. J. Flory. *Macromolecules* **15,** 806 (1982).
7. M. Gottlieb, C. W. Macosko, G. S. Benjamin, K. O. Meyers and E. W. Merrill. *Macromolecules* **14,** 1039 (1981).
8. E. M. Valles and C. W. Macosko. *Macromolecules* **12,** 673 (1979).
9. W. Oppermann and N. Rennar. *Prog. Coll. Polym. Sci.* **75,** 49 (1987).
10. A. L. Andrady, M. A. Llorente and J. E. Mark. *J. Chem. Phys.* **72,** 2282 (1980).
11. A. L. Andrady, M. A. Llorente and J. E. Mark. *J. Chem. Phys.* **73,** 1439 (1980).
12. A. L. Andrady, M. A. Llorente and J. E. Mark. *J. Polym. Sci.; Polym. Phys. Edn* **19,** 621 (1981).
13. J. E. Mark. In *Elastomers and Rubber Elasticity* (edited by J. E. Mark and J. Lal). Am. Chem. Soc., Washington, DC (1982).
14. J. E. Mark. *Pure Appl. Chem.* **53,** 1495 (1981).
15. J. R. Falender, G. S. Y. Yeh and J. E. Mark. *J. Am. chem. Soc.* **101,** 7353 (1979).
16. J. R. Falender, G. S. Y. Yeh and J. E. Mark. *Macromolecules* **12,** 1207 (1979).
17. B. Erman and J. E. Mark. *J. Chem. Phys.* **89,** 3314 (1988).
18. P. G. Higgs and R. C. Ball. *J. Phys. (Fr.)* **49,** 1785 (1989).
19. Y. Termonia. *Macromolecules* **22,** 3633 (1989).
20. Y. Termonia. *Macromolecules* **23,** 1481 (1990).
21. A. Kloczkowski, J. E. Mark and B. Erman. *Macromolecules* **24,** 3266 (1991).
22. J. P. Queslel and J. E. Mark. *Adv. Polym. Sci.* **71,** 229 (1985).
23. J. E. Mark and B. Erman. *Rubberlike Elasticity. A Molecular Primer.* Wiley-Interscience, New York (1988).
24. H. M. James and E. Guth. *J. Chem. Phys.* **15,** 651 (1947).
25. P. J. Flory. *Proc. R. Soc. London, Ser. A.* **351,** 351 (1976).
26. P. J. Flory. *J. Chem. Phys.* **66,** 5726 (1977).
27. B. Erman and P. J. Flory. *J. Chem. Phys.* **68,** 5363 (1978).
28. P. J. Flory and B. Erman. *Macromolecules* **15,** 800 (1982).
29. P. J. Flory. *Polym. J.* **17,** 1 (1985).
30. W. W. Graessley. *Macromolecules* **8,** 186 (1975).
31. W. W. Graessley. *Macromolecules* **8,** 865 (1975).
32. L. M. Dossin and W. W. Graessley. *Macromolecules* **12,** 123 (1979).
33. D. S. Pearson and W. W. Graessley. *Macromolecules* **13,** 1001 (1980).
34. M. Mooney. *J. appl. Phys.* **11,** 582 (1940).
35. R. S. Rivilin. *Philos. Trans. R. Soc. London, Ser. A* **241,** 379 (1948).
36. M. A. Sharaf and J. E. Mark. *J. Macromolec. Sci., Macromolec. Rep.* **A28,** 67 (1991).
37. M. A. Sharaf and J. E. Mark. *Prepr. Polym. Mat. Sci. Engin., Am. Chem. Soc.* **62,** 644 (1990).
38. M. A. Sharaf and J. E. Mark. *Polym. Prepr. Am. Chem. Soc.* **32(1),** 57 (1991).
39. P. J. Flory. *Macromolecules* **15,** 99 (1982).
40. E. M. Valles and C. W. Macosko. *Macromolecules* **12,** 673 (1979).
41. B. Erman and J. E. Mark. *Macromolecules* **20,** 2892 (1987).
42. M.-Y. Tang and J. E. Mark. *Polym. Engng Sci.* **25,** 29 (1985).
43. S. J. Clarson, Z. Wang and J. E. Mark. *Eur. Polym. J.* **26,** 621 (1990).